

85-25888

NASTRAN ANALYSIS COMPARISON TO SHOCK TUBE
TESTS USED TO SIMULATE NUCLEAR OVERPRESSURES

Lt T. K. Wheelless
Nuclear Survivability Group
Analysis Support Branch
ASD/ENSSA
Wright-Patterson AFB, OH 45433

SUMMARY

This report presents a study of the effectiveness of the NASTRAN computer code for predicting structural response to nuclear blast overpressures. NASTRAN's effectiveness is determined by comparing results against shock tube tests used to simulate nuclear overpressures. Seven panels of various configurations are compared in this study. Panel deflections are the criteria used to measure NASTRAN's effectiveness. This study is a result of needed improvements in the survivability/vulnerability analyses capabilities of weapon systems subjected to nuclear blast.

INTRODUCTION

The objective of this project was to research NASTRAN's effectiveness in analyzing nuclear blast overpressure effects on panels as simulated by shock tube tests. Ultimately, this determines NASTRAN's effectiveness in predicting safe panel response to nuclear blast overpressure effects for survivability/vulnerability analysis. Accomplishment of this objective was achieved by comparing NASTRAN data to experimental shock tube test data which the Defense Nuclear Agency (DNA) collected with the Boeing Military Airplane Company under contract DNA-001-76-C-0084 and published in DNA report DNA-4278F, Volumes 1 through 4 (hereinafter addressed as reference 1). Shock tube tests are an accepted method for simulating the effects of nuclear blast overpressures. Therefore, comparing NASTRAN data to shock tube test data is an effective method for validating NASTRAN as an overpressure analysis technique.

NASTRAN is a finite element structural analysis computer code that is universally accepted in the structural analysis community. The version of NASTRAN used in the analysis for this report is COSMIC, a linear analysis valid only for predicting panel response to the yield point. Experimental data used for comparison with NASTRAN came from shock tube tests performed

upon seven panel configurations. These configurations varied in thickness, edge support constraints, magnitudes of subjected overpressures, geometry, and materials (see Table 2 and Figures 13 through 15). Magnitude of first deflection was the criterion used to measure NASTRAN'S effectiveness. Stress was not used as a criterion because deflection data in reference one is of more consistent quality. Deflection and stress exhibit a linear relationship in a material's elastic range. Therefore, deflection is a valid measure of NASTRAN's effectiveness for predicting sure safe panel response. This is discussed in further detail in the Discussion.

Shock tube test are performed by generating a shock wave that propagates down a tube and strikes a specimen. Experimental data used for comparison in this project was performed at Sandia Corporation's THUNDERPIPE shock tube in Albuquerque, New Mexico. The THUNDERPIPE shock tube generates a shock wave by primacord explosives. Figure 1 is taken from DNA report DNA-4278F and illustrates the dimensions of the Thunderpipe Shock Tube. The reader should realize that this is a relatively large test facility.

SHOCK TUBE TEST DATA

Researching NASTRAN's effectiveness for reproducing structural responses observed in shock tube tests required development of the data interpretation methodology introduced in this section. This development is divided into the two subsections: Data Interpretation and Error Effects. Large experimental data fluctuations required development of a data interpretation methodology. This methodology provides a consistent method of interpreting the pressure time history data reported in reference 1. The interpreted data is input into the NASTRAN model built to simulate the tested structure. Error Effects is a study of the effects upon NASTRAN analysis if data contains an inherent interpretational error.

Data Interpretation

Validating any numerical analysis technique requires accurate and consistent methods for reading experimental data used as analytical input data. The following is a methodology developed for reading experimental data of pressure time histories produced in the THUNDERPIPE shock tube. Ideal overpressure curves for reflected pressure time histories are the guidelines for data interpretations.

The reference used for ideal blast waves is: The Effects of Nuclear Weapons, compiled and edited by Samuel Glasstone and Phillip J. Dolan, 3rd edition, published by the United States Department of Defense and the Energy Research and Development Administration (hereinafter addressed as reference 2). Ideal curves for blast waves seldom correlate exactly to experimental shock tube data. Thus, it is emphasized that ideal curves are used only as guidelines. The methodology developed pertains to ideal curves for surface blast waves that strike normal to flat and curved panels. Figure 2 and Definitions of Terms will enhance the reader's understanding of the methodology.

Reflected pressure spikes are the most important consideration when interpreting pressure time history data. Spike peaks and widths are dependent upon post-reflected peaks. Therefore, interpreting experimental

reflected pressure data requires that post-reflected curves be determined first, followed by interpretation of spike peaks and then spike peak widths. Fitted curves will vary from one interpreter to another, but the differences will be negligible if the guidelines for this methodology are followed.

Post-Reflected Curves

Experimental shock wave data exhibits extreme fluxuations in the post-reflected pressure zone (see Figure 3). These fluxuations are due to the combined effects of multiple detonations during ignition of the primacord, close proximity of the test specimen to the explosive, and possible experimental data noise. A realistic approach to analysis requires this data be approximated as a smooth curve. Time steps required to analyse actual experimental data fluxuations would result in unnecessary expenditure of computer time. Selecting the post-reflected curve is accomplished by approximating a least squares fit to the experimental data in the post-reflected pressure zone. The method of least squares is a numerical analysis technique for selecting a particular curve to fit some given data. When approximating a least squares fit, the approach is to maintain an area under the fitted curve that equals the area under the experimental curve. The applicability of this approach to interpreting shock tube test data is verified in Figures 11 and 12 and discussed in Error Effects.

Large data fluxuations in the experimental shock wave data dictate the need for an approximated least squares fit instead of a computational fit. A major characteristic of the actual computational method of least squares is that it puts great emphasis on large fluxuations and little emphasis on small fluxuations. As a result, extreme fluxuations in the recording of data usually dominate the results.

Figure 3 is a typical plot of experimental post-reflected data fitted with the corresponding approximated least squares curve. Note the fitted post-reflected curve follows the general path of the experimental data, while ignoring large fluxuations. Ideal post-reflected curves characteristically exhibit a steady decline in pressure with time; however, experimental curves may decline more erratically as a result of test conditions. Whatever the post-reflected curve profile may be, post-reflected peaks (P_r) always occur at the initial stagnation time (t_s) of the post-reflected zone.

Figures 4 through 6 represent panels that have ideal stagnation times (t_s) of approximately .004 seconds (according to Glasstone calculations). Interpretations of Figures 4 through 6 yield experimental stagnation times (t_s) between .004 seconds and .007 seconds. Ideal stagnation times were used as guidelines to predict ranges where experimental stagnation times should occur.

Spike Peaks

Experimental spike peaks are dependent upon their associated post-reflected pressure peaks. Relationships between spike peaks and unreflected peaks are developed in detail in reference 2. This section develops the general applications of these ideal relationships as applied to experimental pressure data.

Reflected pressure spikes are characteristic of shock waves traveling non-parallel paths relative to the surface which they strike. Ideal spike peaks for reflected shock waves that strike at normal incidence to a flat surface are given by:

$$P_r = 2P(7P_0 + 4P)/(7P_0 + P)$$

Where: P_r = Reflected spike peak (psi)
 P_0 = Ambient pressure, ahead of the shock front (psi)
 P = Peak incident overpressure, behind the shock front (psi)

Peak incident overpressures were read from the experimental data labeled Tunnel Wall Incident Overpressure Time History. It was found that substituting post-reflected peaks (P_s) for peak overpressures (P) yields accurate results for reading the experimental data.

Table 1 lists P_r to P_s relationships within the range of the experimental data. These relationships are used to approximate spike peak magnitudes. Specific magnitudes are determined by the data profiles within the approximated regions. Examples of spike peak readings are given in Figures 4 through 6.

Spike Peak Widths

Reflected pressure spike peak widths are determined by experimental data profiles at the spike peak. Ideal blast waves do not exhibit spike peak widths; however, test conditions can induce this phenomenon. Spike peak magnitude and width are the most important data profiles to be read, since they initiate the greatest structural and material responses. Figures 4 through 6 exhibit data taken from various experimental plots. Corresponding notations define the approach applied in interpreting both spike peak magnitude and width.

Error Effects

Analytical deflections are dependent upon interpretations of the experimental reflected pressure time histories. The interpretation methodology developed in the previous sections is subject to variations from one interpreter to another. Considering these variations, the following study was made to gain some insight to the degree of error induced. This study consists of two approaches as follows: spike peak width variations, and complete displacement of the pressure time histories. Results of this study are covered in Discussion.

Spike peak width variations were analytically applied to a 22"x22"x.193" flat unstiffened panel with 2 sides clamped and 2 sides pinned. A pressure time history was developed for the first shot and the spike peak width was altered for the subsequent shots two and three. These curves were developed solely for the purpose of observation and do not necessarily represent ideal pressure time histories as developed by reference 2. The specific pressure time histories developed are listed with their corresponding plots in Figure 7. Resulting deflections are plotted in Figure 8.

Complete displacement of pressure time histories were studied to observe the effects of general variations in the interpretations of identical shock tube blasts. Actual interpretations were developed by the methodology covered in the section titled Data Interpretation. Ideal interpretations were developed from experimental data measured in the regions of the shock tube walls. These curves were developed for the sole purpose of providing various interpretations for identical shock tube blasts, and do not necessarily represent ideal pressure time histories as developed by reference 2. Two comparisons were made on 22"x22"x.192" flat unstiffened panels, one with all sides clamped and another with all sides hinged. The ideal versus actual interpretations are listed with their corresponding plots in Figures 9 and 11. Resulting deflections are plotted in Figures 10 and 12.

NASTRAN ANALYSIS

A total of seven NASTRAN models were developed to simulate structural response to shock tube overpressur-*s*. NASTRAN models were developed and compared against shock tube tests performed upon four flat panels, one flat stiffened panel, and one honeycomb panel. One curved panel was studied qualitatively since insufficient test data was provided for a quantitative study. The four flat panels and the curved panel were constructed with CQUAD2 elements. For the flat stiffened panel, CQUAD2 elements were used for the skin and CBAR elements were used for the stiffeners. CQUAD1 elements were used to construct the honeycomb panel. Refer to "The Nastran User's Manual" for detailed explanations of these elements. The seven NASTRAN models developed are presented in this section. Refer to Table 2 for general model specifications, Figures 13 through 15 for model geometry. Criterion for building NASTRAN models is simplicity of design. This assures that NASTRAN's effectiveness will be researched from both aspects of economy and accuracy.

Panel deflections are used as the criteria for comparisons between NASTRAN analysis and shock tube data. Stress was not used as a criterion because deflection data in reference one is of more consistent quality. Deflection and stress exhibit a linear relationship in a material's elastic range. Therefore, deflection is a valid measure of NASTRAN's effectiveness for predicting sure safe panel response. This is discussed in further detail in the section titled Discussion. Deflections are compared at panel centers. Tables 3 through 9 list the interpreted pressure time histories for each panel analyzed. Figures 18 through 24 plot the corresponding deflections for each panel. Results of the comparison are also covered in Discussion.

DISCUSSION

Results of the NASTRAN analysis and shock tube test comparisons are listed in Table 10. Results of the error effects studies are listed in Table 11 through 13. First deflections characteristically exhibit the largest deflection responses for aperiodic loading; therefore, magnitudes of first deflections are the comparison criteria. Times of deflections do not dictate stress levels and are therefore considered insignificant.

Percent error between magnitudes of first deflections was the measure of effectiveness in both the NASTRAN versus shock tube comparison and the error effects studies.

A hand calculation shows the correlation between deflection and stress response. The calculation determines edge stress for Panel 1 from NASTRAN's predicted deflection and compares this to edge stress data measured during the shock tube test. Equations are taken from Formulas For Stress and Strain, 5th Ed., Raymond J. Roark and Warren C. Young.

For rectangular plates, all edges fixed,
uniform load over entire plate: $\sigma_{EDGE} = \beta_1 q b^2/t^2$

$$Z_{MAX} = \alpha q b^4/Et^3$$

Where: $\beta_1 = 0.3078$ } Constants for a square plate with
 $\alpha = 0.0138$ } aspect ratio = 1.0
 $q =$ Uniform static load
 $b = 22.0$ in - long edge, all edges the same for panel 1
 $t = .192$ - plate thickness
 $E = 11.0 \times 10^6$ - Youngs modulus
 $\sigma_{EDGE} =$ Maximum stress at edge
 $Z_{MAX} = .219$ in (first deflection maximum).

First, calculate the equivalent static to dynamic uniform load:

$$q = Z_{MAX} E t^3/b^4 \alpha$$

$$q = (.219 \text{ in}) (11.0 \times 10^6 \text{ psi}) (.192 \text{ in})^3/(0.0138) (22.0 \text{ in})^4$$

$$q = 5.27 \text{ psi}$$

Second, calculate maximum stress at the edge:

$$\sigma_{EDGE} = \beta_1 q b^2/t^2$$

$$\sigma_{EDGE} = (-.3078) (5.27 \text{ psi}) (22.0 \text{ in})^2/ (.192 \text{ in})^2$$

$$\sigma_{EDGE} = 21297.18 \text{ psi}$$

Shock tube test edge stress measurements for panel 1 show a maximum value:

$$\sigma_{EDGE} = 25000 \text{ psi}$$

Thus:

$$\% \text{ ERROR} = \left| \frac{\text{NASTRAN} - \text{Test}}{\text{Test}} \right| \times 100$$

$$\% \text{ ERROR} = \left| \frac{21297.18 - 25000}{25000} \right| \times 100$$

$$\% \text{ ERROR} = 14.8$$

This corresponds to a 12.4% error in the deflection comparison for panel 1. Therefore, stress analysis does correlate very closely with deflection analysis, as is expected since stress and deflection exhibit a linear relationship within a materials elastic range.

Stress analysis with NASTRAN requires the appropriate model. Such a model should incorporate a center element and refined elements at the middle of the longest fixed edge of the panel. A center element is required to calculate stress at the panel center. Refined elements at the middle of the longest fixed edge are required to calculate the maximum stress for a fixed edge panel. The refinement of elements is necessitated by the sharp stress gradient that occurs at a panel's fixed edge. Deflection models do not require such element refinement, and therefore require less computer time than stress models. For these reasons deflection was used as the criterion for comparing NASTRAN results with the shock tube tests measurements.

Inherent errors of interpretations of pressure time histories taken from Boeing Military Airplane Company shock tube test data are a source of error in the NASTRAN analysis comparison. The Error Effects section studies two possible error effects. First, a study was conducted to observe the error effects of spike peak width variations. Second, a study was conducted to observe the error effects of completely displacing the pressure time history.

Table 11 list first and second deflections for shots 1, 2, and 3 of the spike peak width study. The term shot refers to a pressure time history. Figure 7 plots the three shots and list their corresponding pressure time histories. Corresponding deflection data is plotted in Figure 8. These are considered reasonable variations of interpretations for spike peaks represented by the Boeing Wichita shock tube test data.

Six possible error effects are taken from this study and the results are listed in Table 12. The procedure of this study observes each shot as an actual and measures the error effect of the two subsequent shots as ideals. Results of this study show that it is reasonable to expect approximately 20% error from a spike peak and 37.4% error in a worse case. It is emphasized here that not all of THUNDERPIPE's pressure time history data is subject to such inherent interpretational error.

Complete displacement of the pressure time history curve is the second error effect study. Figures 9 through 12 plot the pressure time histories and resultant deflections of the two cases. Table 13 list magnitudes for the first and second deflection peaks and their relative percent errors. Times of deflections are not listed since comparisons are made against identical NASTRAN models, which results in identical times of deflections.

Each case represents two interpretations for an identical shock tube test. Observing first deflections, a 39.2% error is found in the worse case.

While this does not represent a reasonable inherent interpretational error of the Boeing Military Airplane Company shock tube data, it is noteworthy in that it emphasizes the effect of the spike peak. Specifically, it takes relatively large variations in interpretations of complete displacements to produce the equivalent error resulting from small variations in interpretations of spike peak characteristics. This follows basic aspects of dynamic structural response for long pulse durations, such as those induced on the panels in this study. The general rule for long pulse durations, those twice the natural period of the oscillator, is that structural response depends primarily on peak pressure and becomes insensitive to impulse.

Results of the comparison between the NASTRAN analysis and shock tube test are listed in Table 10. Figures 18 through 24 plot the corresponding deflections. As aforementioned, percent errors between magnitudes of first deflections are the measurement criteria of effectiveness.

Panels 1 through 4 exhibit very close comparisons between NASTRAN data and shock tube test data -- ranging from 6.5 to 15.3% error. These four panels are flat and homogeneous. They differed in aluminum alloy, panel thickness, boundary constraints, and pressure time histories. Shock tube test data for these four panels were well defined by Boeing Military Airplane Company, and therefore considered to be correctly modeled by NASTRAN.

Trends for error due to modeling techniques cannot be deduced by comparing these four panels. By relating panel descriptions in Table 2 to relative percent errors in Table 10, it is determined that neither boundary constraints, panel thickness, or material properties are proportional to magnitude of error.

Panels 5 and 6 are flat nonhomogeneous panels. Panel 5 is a honeycomb construction and panel 6 is a stiffened panel. Shock tube test data for panel 5 was well defined by Boeing Wichita, and therefore considered to be correctly modeled by NASTRAN. Accordingly, panel 5 exhibits a very close comparison at 7.2% error. Panel 6 exhibits the worst case for deflection comparisons at 42.69% error.

Factors that may have affected the results of panel 6 are: incorrect boundary conditions, inherent interpretational error of the pressure time history, and exceeding the linear analysis capabilities of NASTRAN. This panel was modeled with boundary constraints as stated in the Boeing Wichita final report. Since deflection frequencies between the NASTRAN and shock tube test data coincide, it is assumed that boundary conditions are defined reasonably well. Inherent interpretational errors of pressure time histories have been addressed in the study on error effects and show that considerable error can be induced. NASTRAN uses linear finite element analysis, making it reliable in the elastic range of a material's response. Table 3 shows that panel 6 was subjected to a maximum reflected overpressure of 4.75 psi. Plastically yielding deflections during shock tube test exhibit substantially larger deflection magnitudes than NASTRAN, since NASTRAN continues linear past the yield point on the stress strain curve. Boeing Military Airplane Company documents that panel 6 plastically deformed during four shock tube tests. Figure 23 indicates that plastic deformation may have occurred during this shot; verifying the possibility that NASTRAN's elastic limits may have been exceeding.

Panel 7 is used for qualitative comparisons only, since there is no experimental deflection data available. It is a curved homogeneous panel which was subjected to a maximum overpressure of 10.5 psi -- the largest of all panels studied. Figure 24 shows the deflection response predicted by NASTRAN. The magnitude of the first deflection is relatively small, at .043 inches, for the size of reflected pressure experienced. This coincides reasonably with Boeing Military Airplane Company documentation that panel seven exhibited no permanent deformation after the test.

CONCLUSIONS

- (1) NASTRAN is an accurate analysis code for predicting elastic structural response to shock tube tests used to simulate nuclear blast overpressure effects.
- (2) Accurate pressure time histories of shock blast are extremely vital for accurate predictions of structural response.
- (3) NASTRAN's modeling flexibilities allow for greater analysis capabilities of nuclear blast overpressure effects than are allowed with present nuclear effects analysis codes.
- (4) NASTRAN's programming efficiency results in less computer time required than with present nuclear effects analysis codes.
- (5) NASTRAN's accuracy in overpressure analysis requires accurate model generation, which is dependent upon accurate structural and load input data.

P_s (psi)	P_r (psi)
.1	$2.01 \times P_s$
1	$2.06 \times P_s$
5	$2.28 \times P_s$
10	$2.53 \times P_s$

Table 1 - P_r to P_s relationships for approximating spike peak magnitudes.

	PANEL DESCRIPTION	ALUMINUM MATERIAL	DENSITY $\frac{\text{lb. sec}^2}{\text{in}^4}$	POISSON'S RATIO	MODULUS ELASTICITY (psi)	BOUNDARY CONDITIONS	YIELD STRENGTH (psi)	ULTIMATE STRENGTH (psi)
PANEL 1	22" x 22" x.192" Flat	6061-T6	2.54×10^{-4}	.33	11.0×10^6	4 Sides Clamped	40,350	44,820
PANEL 2	22" x 22" x.192" Flat	6061-T42	2.54×10^{-4}	.33	10.4×10^6	4 Sides Clamped	18,410	36,090
PANEL 3	22" x 22" x.193" Flat	6061-T6	2.54×10^{-4}	.33	10.9×10^6	2 Sides Clamped/ 2 Sides Pinned	40,500	45,200
PANEL 4	22" x 22" x.315" Flat	6061-T42	2.54×10^{-4}	.33	10.6×10^6	4 Sides Clamped	19,380	37,810
398 PANEL 5	22" x 22" x.333" Honeycomb	5052-0 Face Sheets (1)	2.54×10^{-4}	.33	12.3×10^6	4 Sides Pinned	13,270	30,300
PANEL 6	36" x 39" x.0625" Flat Stiffened	2024-T3511 Stiffeners 2024-T3 Skin (2)	2.59×10^{-4}	.33	10.6×10^6	2 Sides Clamped/ 2 Sides Pinned	52,230	66,320
PANEL 7	36" x 22.8" x.08" Curved	6061-T6	2.54×10^{-4}	.33	10.9×10^6	4 Sides Clamped	40,500	45,200

(1) Refer To Fig. 16

(2) Refer To Fig. 17

MODEL SPECIFICATIONS

TABLE 2

PANEL 1	
TIME (sec)	PRESSURE (psi)
0.0	0.0
0.0003	3.0
0.0015	3.3
0.0029	1.7
0.0042	1.6
0.0125	1.95
0.018	1.4
0.031	1.15
0.046	1.0

TABLE 3

PANEL 2	
TIME (sec)	PRESSURE (psi)
0.0	0.0
0.0002	1.2
0.002	0.6
0.006	0.5
0.0125	0.45
0.0212	0.42
0.0302	0.4
0.0352	0.4
0.0432	0.37

TABLE 4

PANEL 3	
TIME (sec)	PRESSURE (psi)
0.0	0.0
0.00025	1.3
0.002	0.98
0.0035	0.7
0.006	0.45
0.013	0.35
0.0225	0.35
0.0285	0.3
0.0395	0.25
0.044	0.2

TABLE 5

PANEL 4	
TIME (sec)	PRESSURE (psi)
0.0	0.0
0.0003	0.9
0.0017	2.0
0.003	1.0
0.0054	0.88
0.0115	0.75
0.017	0.67
0.025	0.63
0.031	0.6
0.04	0.6

TABLE 6

PANEL 5	
TIME (sec)	PRESSURE (psi)
0.0	0.0
0.0003	1.38
0.002	1.1
0.0035	0.8
0.0047	0.66
0.006	0.62
0.0095	0.58
0.0205	0.54
0.028	0.52
0.034	0.5

TABLE 7

PANEL 6	
TIME (sec)	PRESSURE (psi)
0.0	0.0
0.0002	2.4
0.0015	4.75
0.002	2.25
0.0045	1.4
0.012	1.2
0.026	1.0
0.04	0.09

TABLE 8

PANEL 7	
TIME (sec)	PRESSURE (psi)
0.0	0.0
0.0002	6.7
0.001	10.5
0.0029	5.9
0.0032	5.0
0.0044	4.4
0.015	3.7
0.027	2.9
0.033	2.5

TABLE 9

Tables 3 - 9:
Pressure Time Histories
input into NASTRAN
for Panels 1 - 7

1st and 2nd Peak Deflections

Panel/ Defl.	Magnitude (inches)			Time (sec)		
	NASTRAN	Test	% Error (1)	NASTRAN	Test	% Error (1)
1/1st	.219	.250	12.4	.0035	.0030	16.7
1/2nd	-.088	-.160	45.0	.0070	.0065	7.7
2/1st	.173	.150	15.3	.0060	.0044	36.4
2/2nd	-.040	-.065	38.5	.0130	.0090	44.4
3/1st	.113	.130	13.1	.0040	.0040	0.0
3/2nd	-.059	-.067	11.9	.0085	.0080	6.3
4/1st	.029	.031	6.5	.0025	.0030	16.7
4/2nd	-.012	-.009	33.3	.0050	.0055	9.1
5/1st	.154	.166	7.2	.0018	.0032	43.8
5/2nd	-.039	-.060	35.0	.0036	.0057	36.8
6/1st	.066	.115	42.6	.0025	.0032	21.9
6/2nd	-.042	-.030	40.0	.0060	.0055	9.1
7/1st	.043	(2)	—	.0025	(2)	—
7/2nd	-.015			.0045		

$$(1) \% \text{ Error} = \left| \frac{\text{NASTRAN} - \text{Test}}{\text{Test}} \right| \times 100$$

(2) Test Data Not Available

Table 10

Spike Peak
Width Effects
(1st and 2nd Deflection Peaks)

Shot/ Defl.	Time (sec)	Defl. (inches)
1/1st	.0039	.1412
1/2nd	.0084	-.0572
2/1st	.0039	.1779
2/2nd	.0084	-.0928
3/1st	.0045	.1940
3/2nd	.0086	-.1091

Table 11

Spike Peak
Width Effects
(1st Deflection)

Shot Ideal/Actual	% Error (1)
1/2	20.6
1/3	27.2
2/1	26.0
2/3	8.3
3/1	37.4
3/2	9.1

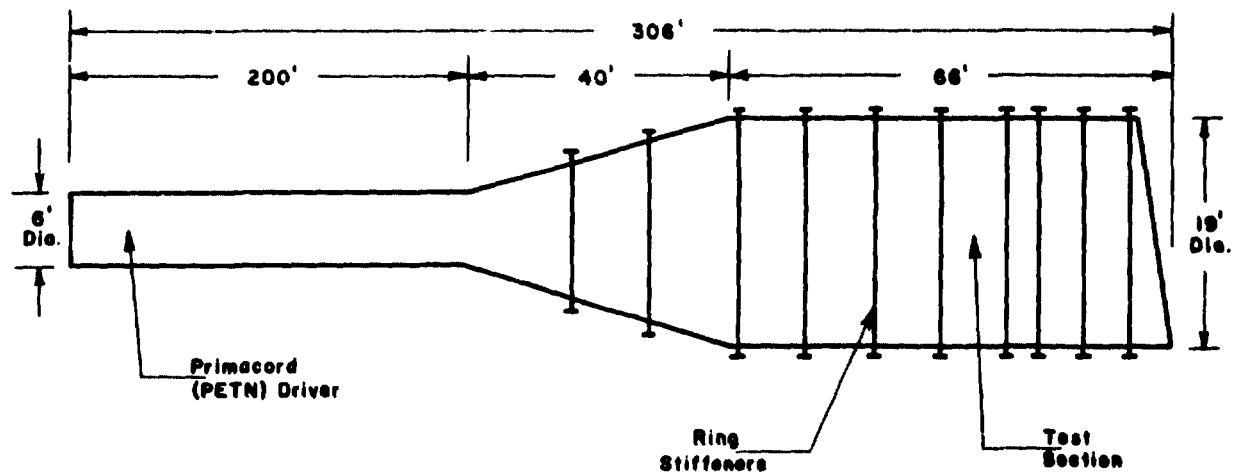
Table 12

Complete Displacement Effects
(1st and 2nd Deflections)

Case/ Defl.	Ideal Defl. (inches)	Actual Defl. (inches)	% Error (1)
1/1st	.2162	.219	1.3
1/2nd	-.0656	-.088	25.5
2/1st	.2408	.173	39.2
2/2nd	-.0739	-.040	84.8

Table 13

$$(1) \% \text{ Error} = \left| \frac{\text{Ideal} - \text{Actual}}{\text{Actual}} \right| \times 100$$



THUNDERPIPE SHOCK TUBE

Figure 1 - Sandia Corporation's THUNDERPIPE shock tube

DEFINITIONS OF TERMS

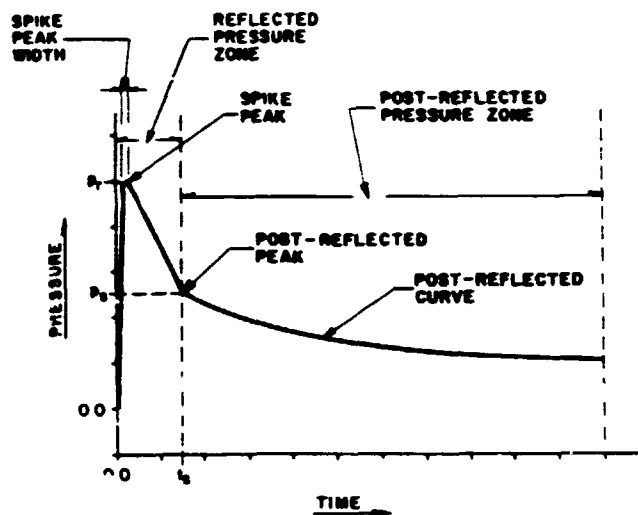
Reflected Pressure (P_r) - The initial pressure experienced by surfaces subjected to shock waves striking at non-parallel paths relative to the surface, resulting in a greater pressure experienced by the surface than is present at the shock front.

Reflected Pressure Time History - A numerical account (tabular or graphical) of the pressure as a function of time experienced by a surface subjected to shock waves traveling non-parallel paths relative to the surface. It is the addition of incident overpressure, dynamic pressure, and reflected pressure effects.

Stagnation Time (t_s) - The time at which reflected pressure effects subside, leaving only incident overpressure and dynamic pressure effects. It is a function of panel geometry and shock wave velocity. Ideal t_s is calculated from reference 2.

Stagnation Pressure (P_s) - The post-reflected peak pressure that corresponds to stagnation time (t_s).

Ideal Pressure Curve - Developed in reference 2. Major characteristics are an initial reflected pressure effect until time t_s , followed by a steady and more gradual decrease of the post-reflected pressure.



**TYPICAL REFLECTED PRESSURE
TIME HISTORY CURVE**

Figure 2 - A typical curve fitting of a reflected pressure time history from the Boeing Wichita shock tube test data.

ORIGINAL PAGE IS
OF POOR QUALITY.

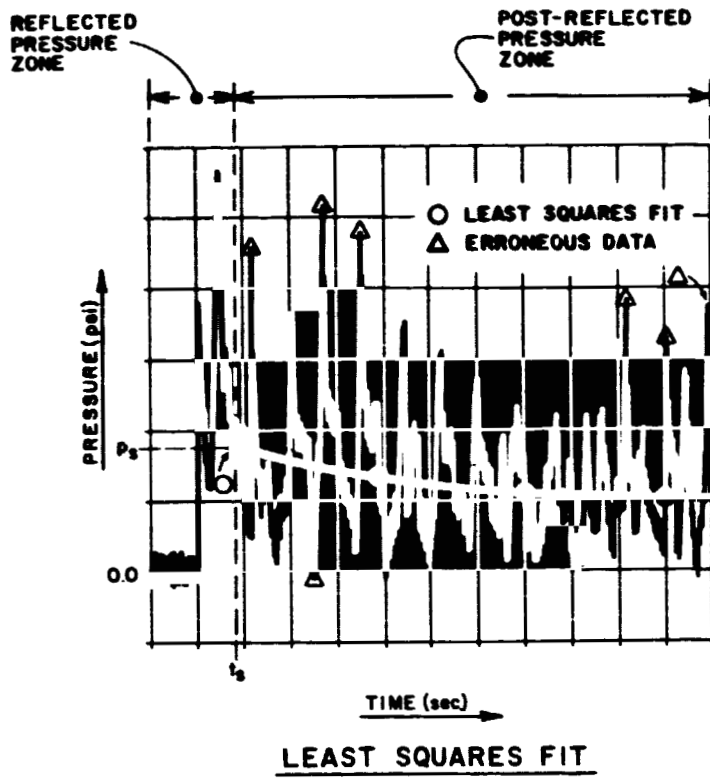
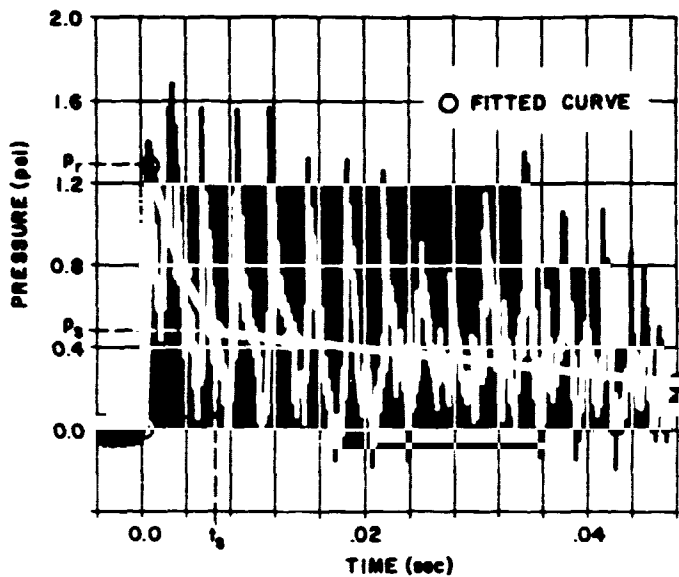


Figure 3 - Approximated least squares fit on a typical plot of experimental post-reflected data.

ORIGINAL PAGE IS
OF POOR QUALITY

INTERPRETATIONS



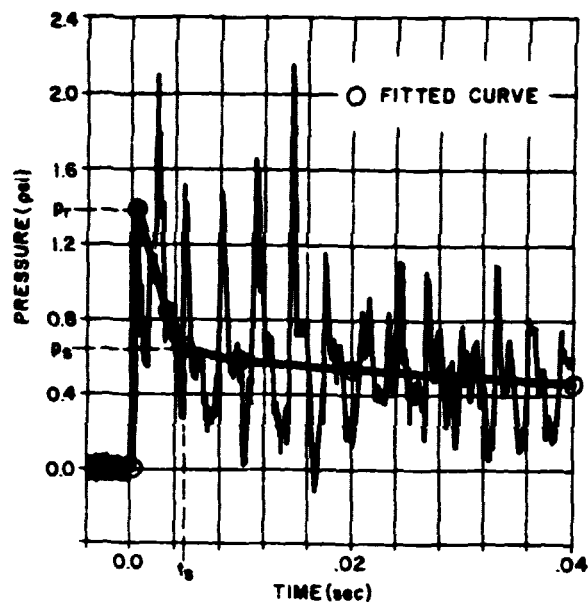
REFLECTED PRESSURE TIME HISTORY

Figure 4 - An example of data interpretation.

Curve Fitting for Figure 4

Apply a least squares approximation to curve fit post-reflected data. Note that experimental data fluxuations subside around .028 seconds, giving an indication of where the optimum approximated pressure levels are for the fitted curve. The post-reflected peak (P_s) is interpreted to be 0.5 psi at an experimental stagnation time (t_s) just over .006 seconds.

Table 1 indicates the reflected peak (P_r) is approximately 1.2 psi. Therefore, the initial experimental peak is taken as P_r at 1.3 psi and the second experimental peak is disregarded since it is well above the expected range of P_r . Fitting only one point in the range of P_r results in the absence of a spike peak width.



REFLECTED PRESSURE TIME HISTORY

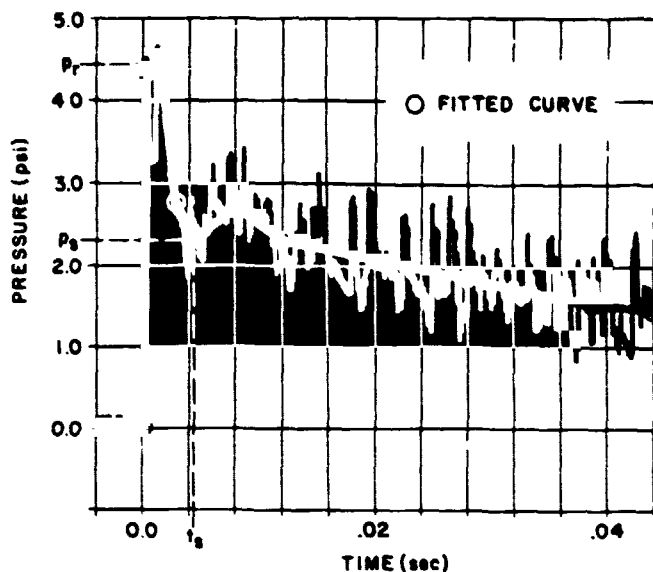
Figure 5 - An example of data interpretation.

Curve Fitting for Figure 5

Approximate a least squares curve to fit post-reflected data. Experimental data fluctuations subside around 0.022 seconds and 0.03 seconds, giving an indication of optimum fitted curve pressure levels. There are several data fluctuations before 0.016 seconds that are ignored. The post-reflected peak (P_s) is interpreted to be approximately .65 psi, corresponding to an experimental stagnation time (t_s) around .005 seconds.

Calculating the reflected peak yields P_r approximately equal to 1.3 psi - refer to Table 1. The initial experimental peak is recorded as P_r at 1.4 psi and the second experimental peak is disregarded since it is not within the expected range of P_r . There is no spike width because only one point is fitted in the range of P_r .

ORIGINAL SOURCE
OF POOR QUALITY



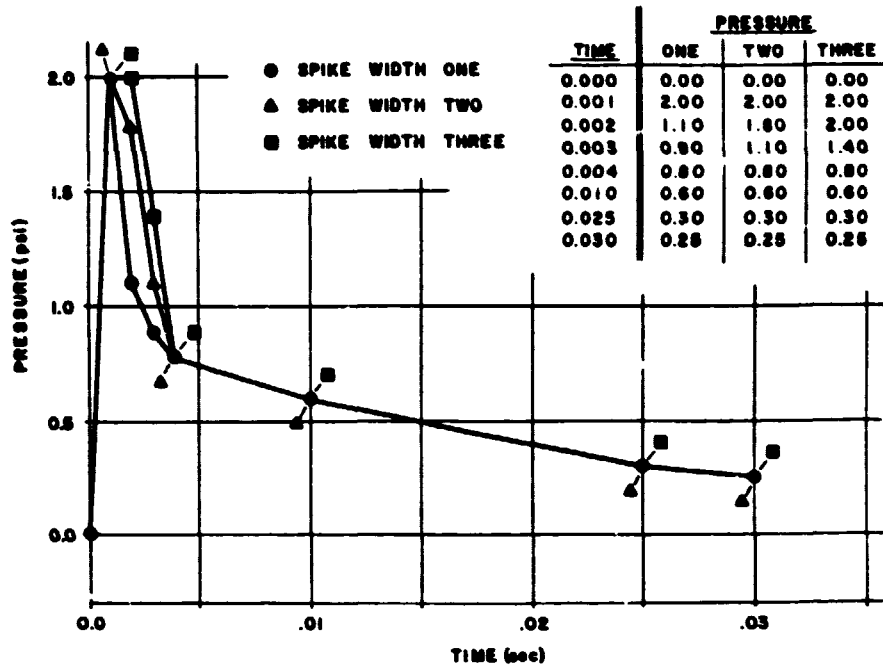
REFLECTED PRESSURE TIME HISTORY

Figure 6 - An example of data interpretation.

Curve Fitting for Figure 6

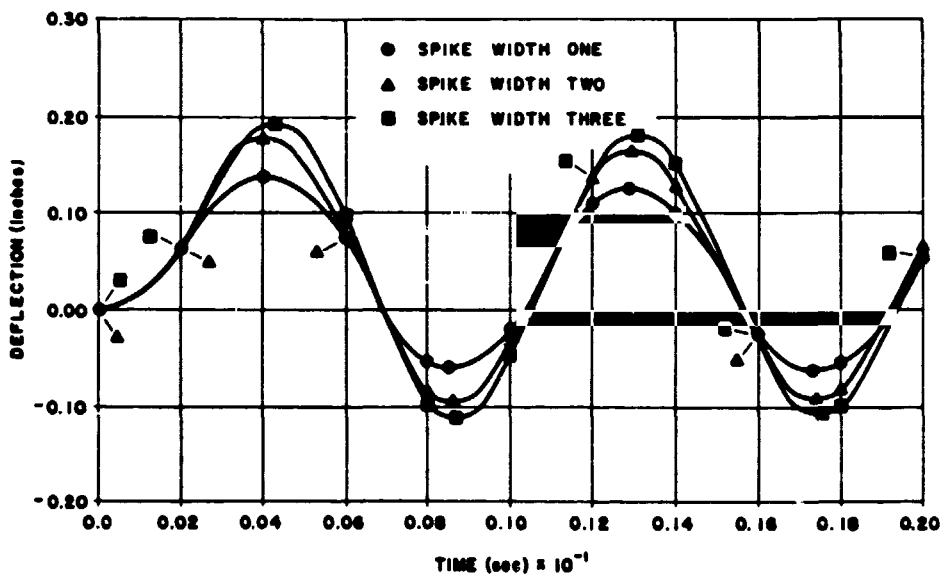
Curve fit the post-reflected data with a least squares approximation. Post-reflected data clearly deviates from theory between t_s and 0.012 seconds. This is shock tube phenomenon and is recorded as fitted data since project objectives are to validate NASTRAN against shock tube test. Near 0.032 seconds experimental data fluxuations subside, giving an indication of optimum approximate pressure levels for the fitted curve. The post-reflected peak (P_s) is interpreted to be approximately 2.3 psi, corresponding to an experimental stagnation time (t_s) .0045 seconds. Note that P_s is defined as the initial pressure of the post reflected curve.

Table 1 approximates the reflected peak P_r at 4.5 psi. Experimental data contains two points at this pressure range; therefore, a spike width does exist as indicated by the fitted curve. This deviates from the ideal but is recorded in order to duplicate shock tube phenomenon. Smooth spike peak widths are fitted and experimental data fluxuations at the peak are disregarded.



PRESSURE TIME HISTORIES

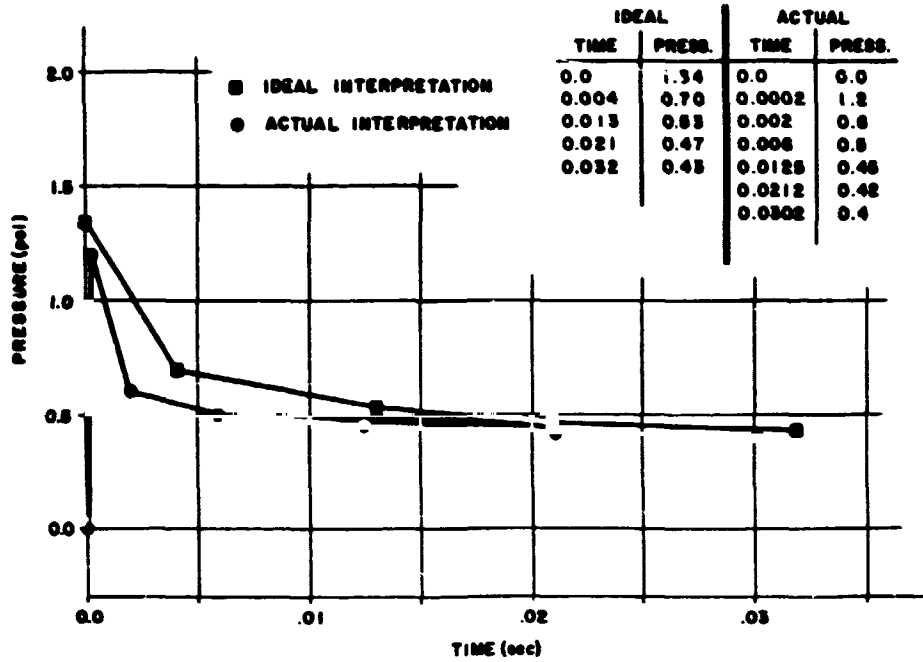
Figure 7 - Error Effects Study #1. Spike peak width interpretation variations.



SPIKE WIDTH DEFLECTION EFFECTS

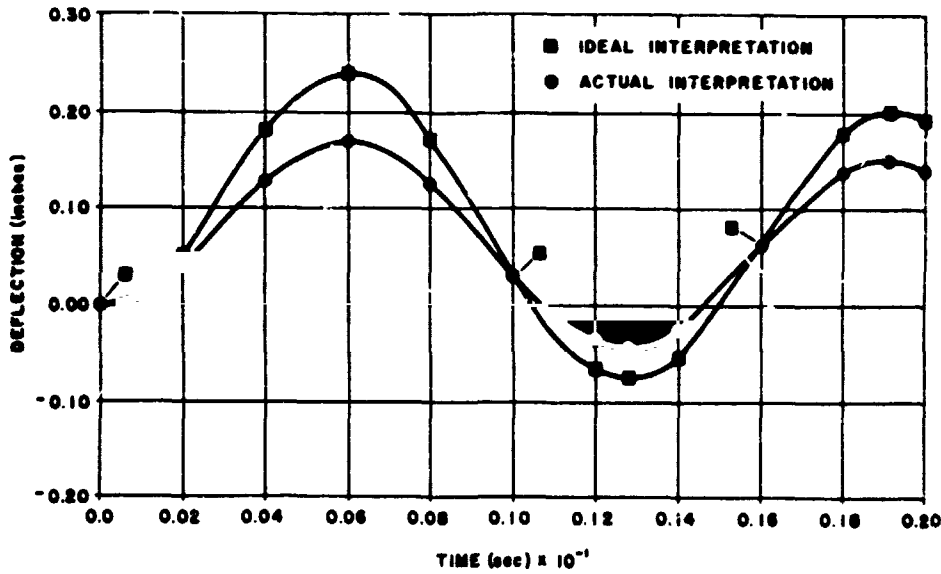
Figure 8 - Error effect study #1. Deflections resulting from pressures depicted in Figure 7.

ORIGINAL PAGE IS
OF POOR QUALITY



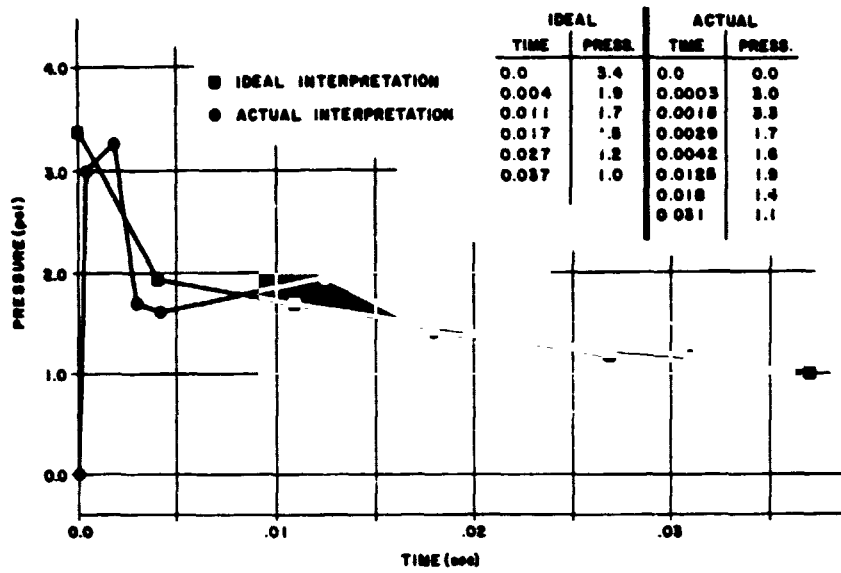
PRESSURE TIME HISTORIES

Figure 9 - Error effect study #2. Complete displacement interpretation variation.



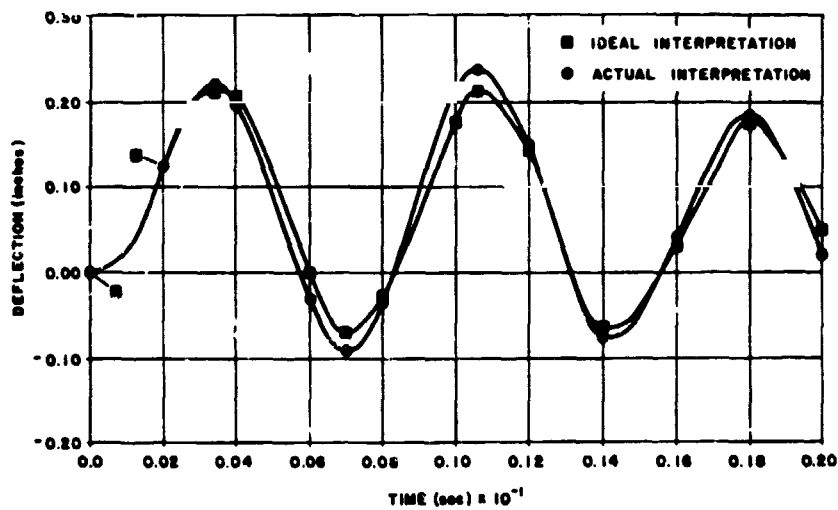
IDEAL vs. ACTUAL DEFLECTIONS

Figure 10 - Error effects study #2. Deflections resulting from pressures depicted in Figure 9.



PRESSURE TIME HISTORIES

Figure 11 - Error effects study #3. Complete displacement interpretation variation.



IDEAL vs. ACTUAL DEFLECTIONS

Figure 12 - Error effects study #3. Deflections resulting from pressures depicted in Figure 11.

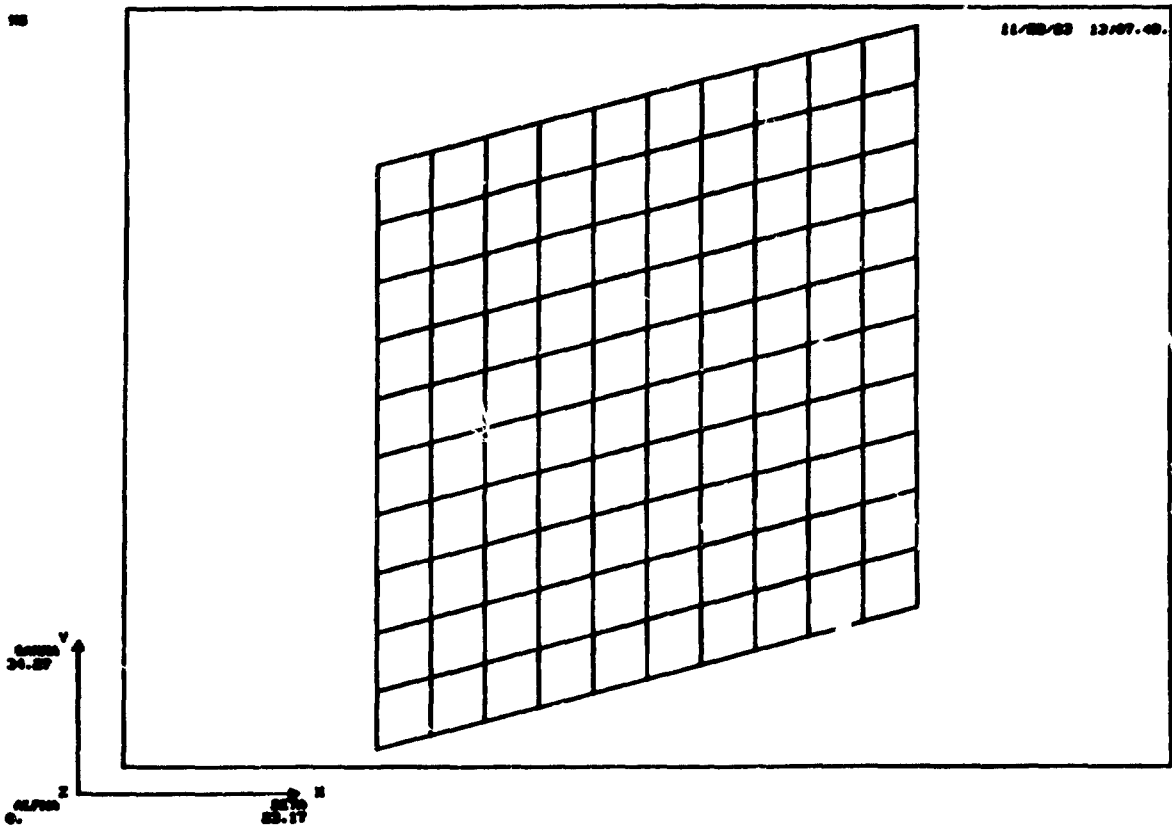


Figure 13 - NASTRAN finite element model for Panels 1 through 5. Refer to Table 2 for specific panel characteristics.

ORIGINAL PAGE IS
OF POOR QUALITY

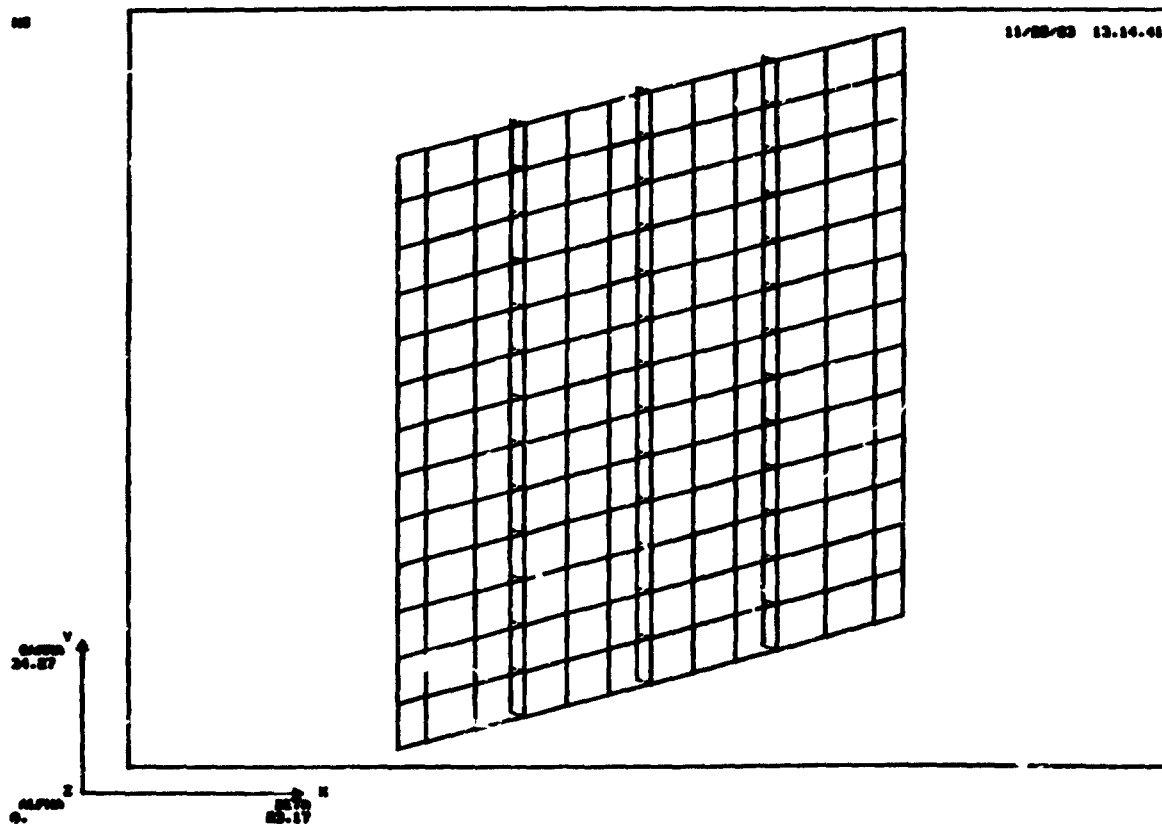


Figure 14 - NASTRAN finite element model for Panel 6, a flat stiffened panel. Refer to Table 2 for specific panel characteristics.

ORIGINAL PAGE IS
OF POOR QUALITY

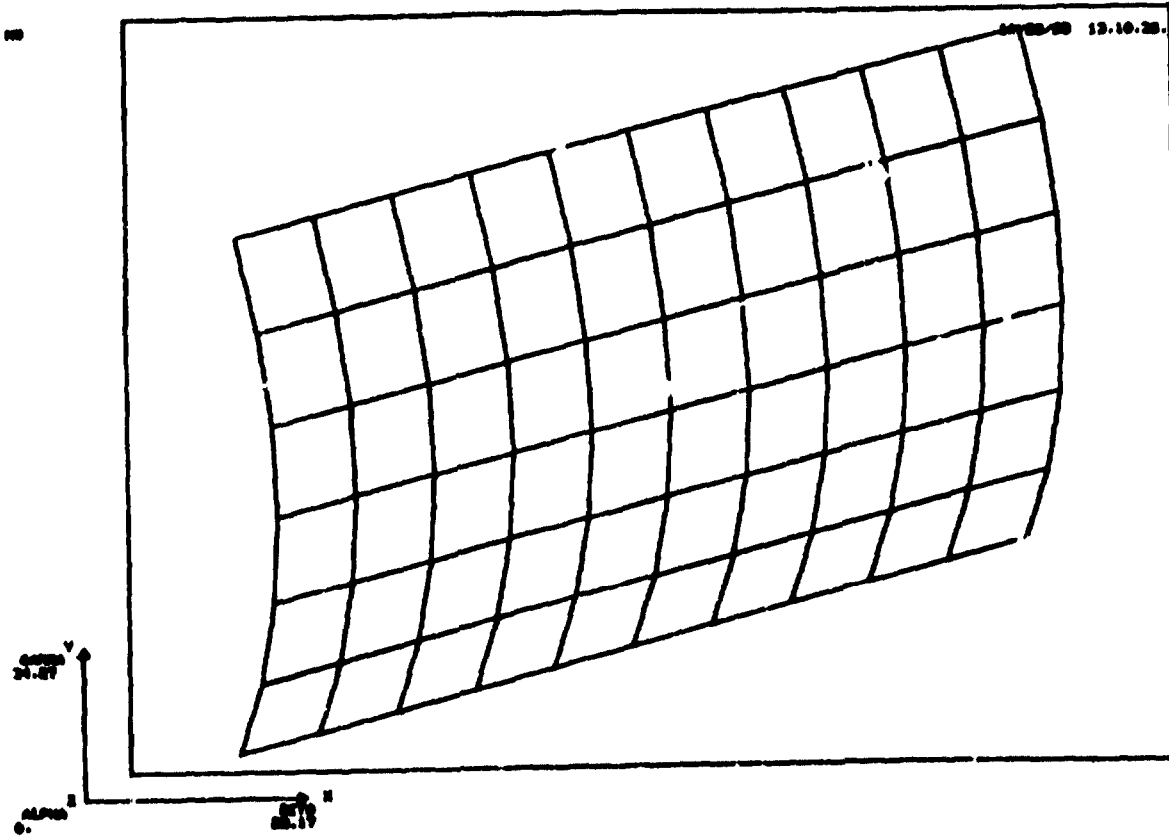
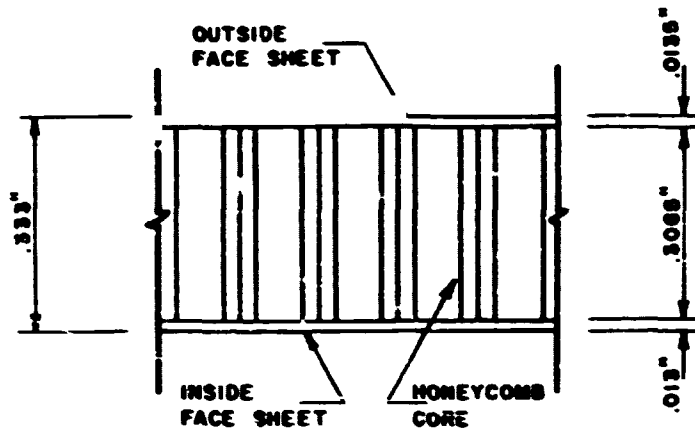
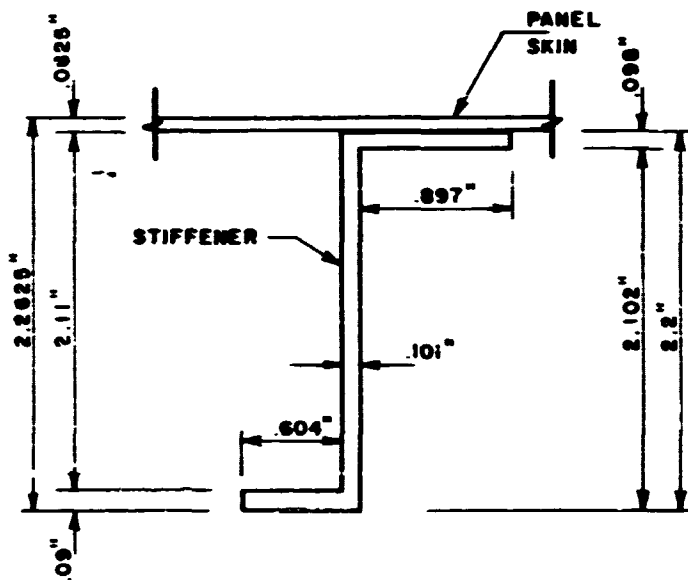


Figure 15 - NASTRAN finite element model for Panel 7, a curved panel. Refer to Table 2 for specific panel characteristics.



PANEL 5
CROSS SECTION

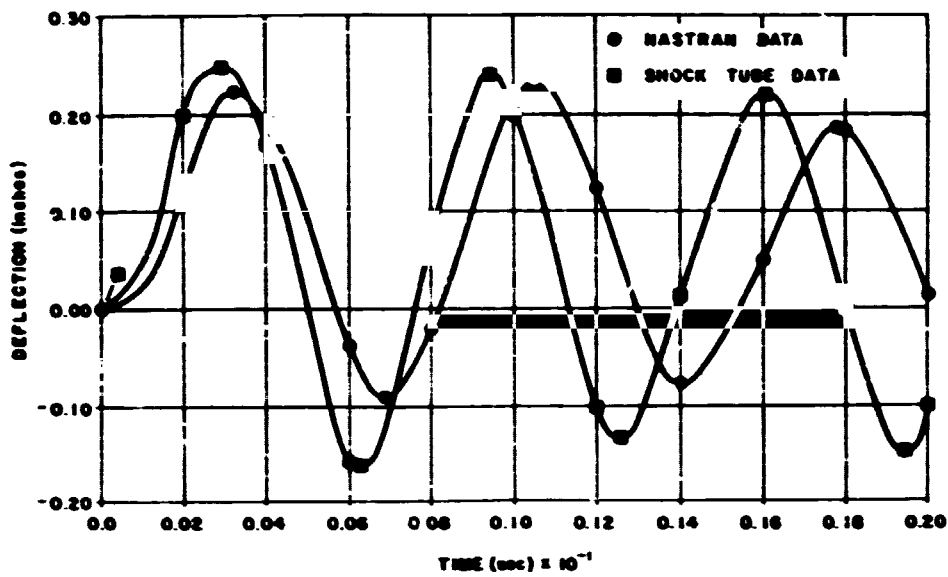
Figure 16



PANEL 6
STIFFENER CROSS SECTION

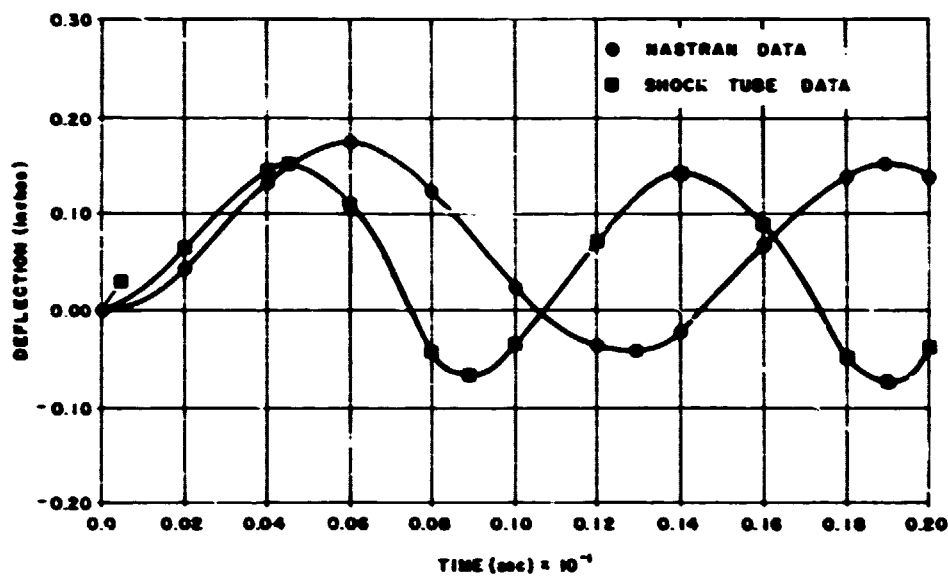
Figure 17

ORIGINAL PANEL 18
OF POOR QUALITY



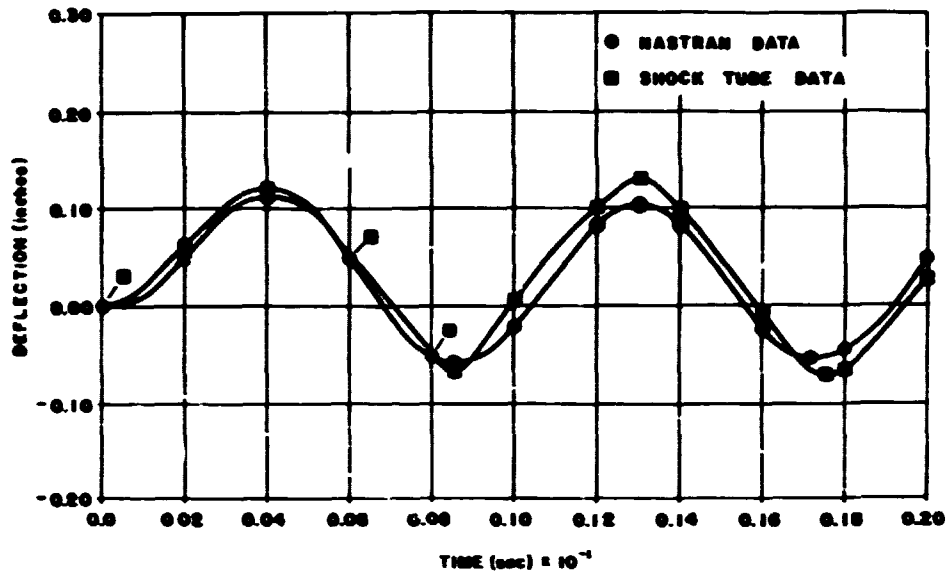
PANEL ONE

Figure 18 - NASTRAN versus shock tube deflections.



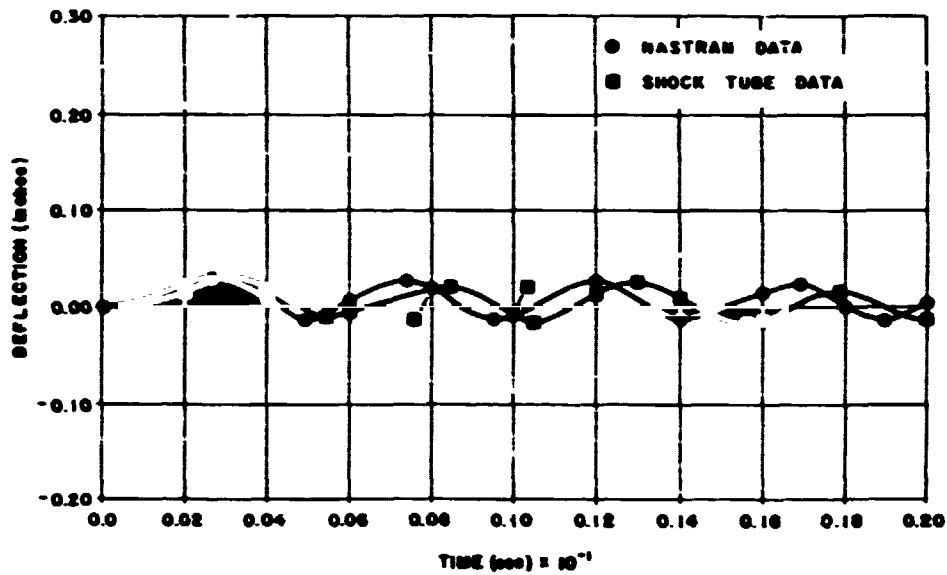
PANEL TWO

Figure 19 - NASTRAN versus shock tube deflections.



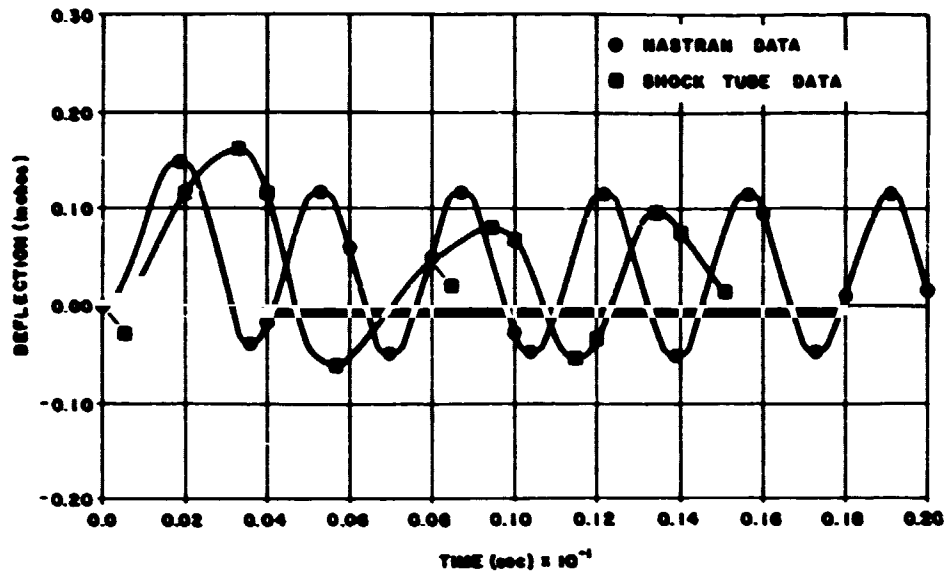
PANEL THREE

Figure 20 - NASTRAN versus shock tube deflections.



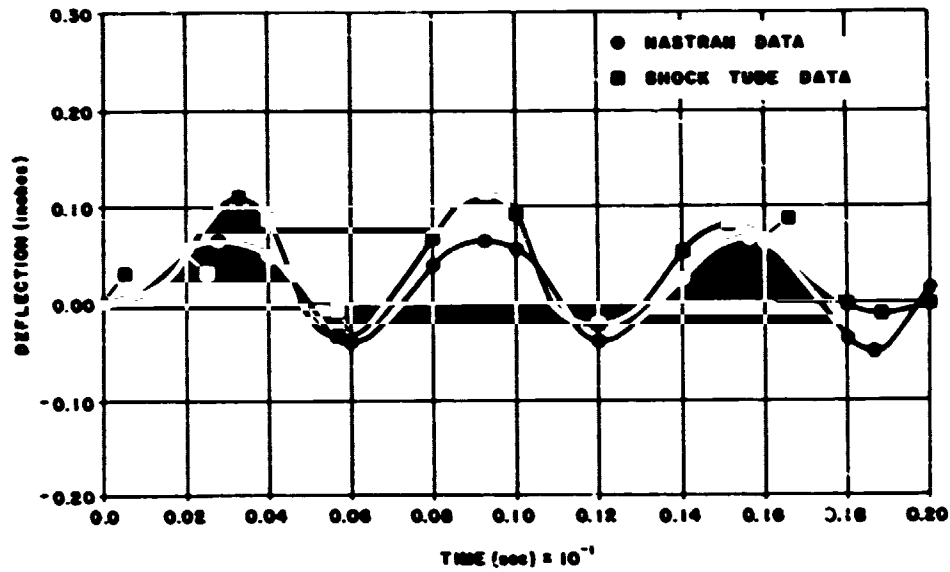
PANEL FOUR

Figure 21 - NASTRAN versus shock tube deflections.



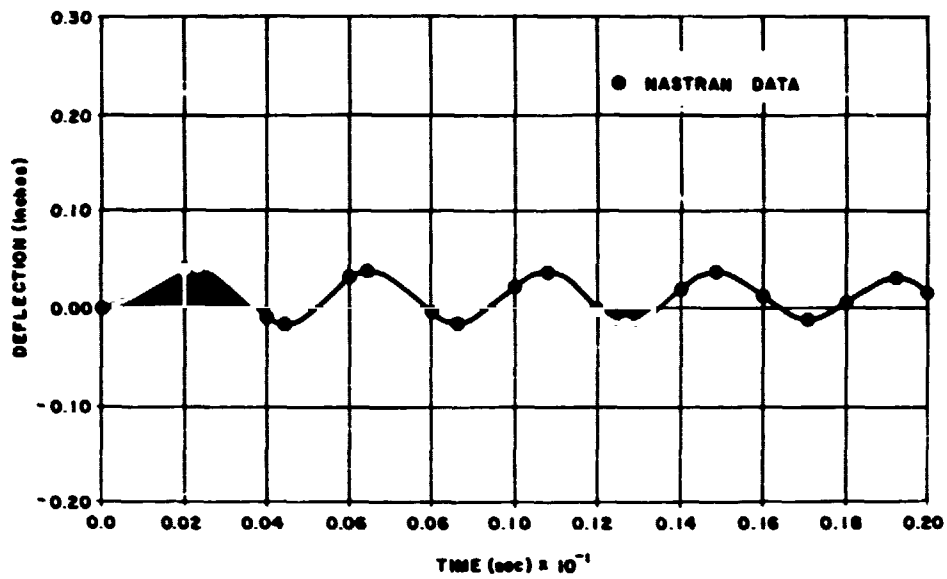
PANEL FIVE

Figure 22 - NASTRAN versus shock tube deflections.



PANEL SIX

Figure 23 - NASTRAN versus shock tube deflections.



PANEL SEVEN

Figure 24 - NASTRAN analysis deflection.